Simulating magnetic field evolution in isolated neutron stars

Ankan Sur[1]

1. Nicolaus Copernicus Astronomical Center, Polish Academy of Sciences, Bartycka 18, 00–716 Warsaw, Poland

We present results for magnetohydrodynamical simulations of evolving neutron stars in the first moments of its lifetime. We study the poloidal field instability and how the magnetic field components change with time. We find that although our final field does not reach a stable equilibrium, it settles to a twisted torus geometry with a dominant poloidal component and a weaker toroidal field reaching 10% of the total magnetic energy at 40 ms. However, at much later evolution times ($t \sim 450$ ms), the toroidal field reduces to 1% of the total magnetic energy.

1 Introduction

Neutron stars (NS) are extremely dense compact objects exhibiting the strongest magnetic fields known to date in the universe. The surface field strength is typically 10^{12} G for ordinary NSs and above 10^{15}G for magnetars. Despite such estimates for the strength of the magnetic field, its structure is not completely understood. Polarimetric studies of pulsar radio emission have enabled us to probe the shape of pulsar magnetospheres. These observations indicate that magnetism is predominantly dipolar (Chung & Melatos, 2011a,b). NICER has recently observed in X-rays that the field at the surface is not an aligned dipole, but rather an intricate multipolar structure (Bilous et al., 2019).

In addition to the external field topology, observations of the internal field topology are even more difficult, but are thought to be fundamental to understanding the nature and strength of electromagnetic and gravitational wave emission from the star (Thompson & Duncan, 1996; Cutler, 2002). In fact, as gravitational-wave astronomy advances, it may be possible to detect magnetic field topologies by using gravitational waves (Lasky & Melatos, 2013). Therefore, obtaining a theoretical understanding of the interior field as well as exploring its nature through numerical simulation is of great importance.

A number of studies have investigated the balance of the Lorentz force and gravity within magnetic main sequence stars and white dwarfs, e.g. for the axisymmetric case by (Braithwaite & Nordlund, 2006) and a similar non-axisymmetric study by (Braithwaite, 2008). For the NS case, equilibrium solutions in Newtonian gravity were obtained by Haskell et al. (2008); Lander & Jones (2009) and Sur et al. (2020) and in general relativity by Kiuchi & Yoshida (2008); Ciolfi et al. (2010) and Sur et al. (2022). A purely poloidal field undergoes the so-called "Taylor instability" and is thus unstable. The instability in NSs has been studied numerically in general relativity by Ciolfi et al. (2011); Lasky et al. (2011) and Ciolfi & Rezzolla (2012). They find that an initially poloidal field becomes unstable at a Alfvén crossing timescale, and toroidal components of the field emerge. Often, equilibrium configurations are

approximated by a twisted-torus configuration, in which a toroidal component stabilizes the poloidal field (Braithwaite & Nordlund, 2006) or a *tilted-torus* configuration (Lasky & Melatos, 2013).

There are still questions, however, as to how the field will ultimately develop. Specifically, while it is clear that a mixed field is necessary, the relative strength of the components cannot be determined from the study of equilibrium configurations since these configurations typically allow for some degree of flexibility in adjusting this parameter (Glampedakis & Lasky, 2016). Models can thus be obtained with toroidal fields that are from a few percent (Lander & Jones, 2009) to more than an order of magnitude stronger than those with polioidal components (Ciolfi & Rezzolla, 2013).

In view of the fact that most hydromagnetic instability studies have focused on setting up equilibrium configurations based on a specific geometry, it is essential to investigate the non-linear evolution of NSs for a variety of topologies and to define a barotropic EOS, not only to determine whether the field is unstable, but also what the final state determined by the non-linear saturation of the instability will be. These issues are crucial to grasp, since the field configuration of a NS plays a crucial role in attempts to determine the mass and radius of the star from X-ray observations, and in determining the gravitational wave emission properties of the system (Lasky, 2015).

Here, we provide nonlinear magnetohydrodynamical (MHD) and General Relativistic MHD simulations of magnetised NSs to explore the instability, the global evolution, and the final configuration of the magnetic field. Neither superfluidity nor superconductivity are considered in modeling the star's core or crust. We made these choices partly for convenience, but also due to the fact that instabilities on dynamical time scales determine the field's configuration shortly after the NS is born. Various setups and initial conditions are explored, allowing for fields with initially stronger poloidal or toroidal components.

2 Method

We use the publicly available code `PLUTO` (Mignone et al., 2007) to solve the Newtonian MHD equations and the `Athena++` code (White et al., 2016) to solve the GRMHD equations.

The MHD equations have closure with a barotropic EOS of $p = p(\rho)$, which we assume to be an $n = 1$ polytrope. Using a static grid, we calculate the pressure using the EOS and the density (thereby maintaining the barotropy of the system), in a spherical coordinate system in three dimensions. We have a resolution of $\Delta r \sim 0.19$ km inside the star, while we have a resolution of $\Delta r \sim 0.25$ km in the atmosphere. Using a piece-wise parabolic function, the interpolations are accurate to second order in space. We use Runge Kutta 3 (RK3) time stepping with a Courant-Friedrichs-Lewy limit of 0.3. For computing fluxes, we use a Harten-Lax-van Leer (HLL) Riemann solver. By using the hyperbolic divergence cleaning method, the solenoidal constraint $\nabla \cdot B = 0$ is maintained. The gravitational potential of a star in different regions is calculated analytically and provided as an input, and it does not change with time. Density distribution of stars is, however, only weakly affected by magnetic fields, which is generally a good approximation (Haskell et al., 2008).

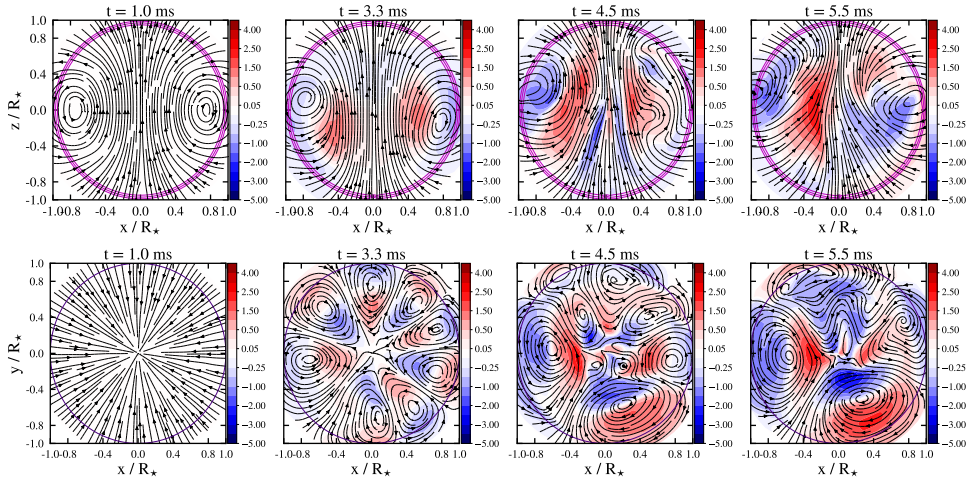

Fig. 1: Magnetic field lines from MHD simulation (*top*) meridoinal view (*bottom*)equatorial view. The colorscale shows the strength of toroidal field in units of 10^{15} G. (figure from Sur et al. (2020))

3 Results

The evolution of the magnetic field occurs on a characteristic timescale associated with the system, called the Alfvén crossing time, which is given by

$$\tau_{\rm A} = \frac{2R\sqrt{4\pi\langle\rho\rangle}}{\langle B\rangle}, \tag{1}$$

where $\langle..\rangle$ represents volume averaged quantities. For $\langle B\rangle \sim 4.5\times10^{15}$ G, we obtain $\tau_{\rm A} \sim 12$ ms. Theoretically, we should expect the field to rearrange itself after one Alfvén timescale, as we shall see it indeed does in our simulations. We will discuss two main issue here. First is the poloidal field instability and the growth of the toroidal component. And second is the energies of the poloidal and toroidal field, and conservation of energy in the star.

3.1 Poloidal field instability

Our purely poloidal field is unstable and this gives rise to a toroidal component inside the star. We plot the two-dimensional projections of the magnetic field lines on the x-y plane (equatorial view) and the x-z plane (meridional view) in Fig. 1 with the title representing the different time stamps. The strength of the toroidal field in Gauss is given by the colorbar. In the beginning of evolution, the field lines' cross-sectional area first changes, which corresponds to the so-called varicose mode. Following this is the transverse displacement of the fluid along the neutral line, which leads to the development of the "kink" instability (Lander & Jones, 2011; Lasky et al., 2011).

In the system, the initial axisymmetry is replaced by a nonaxisymmetric structure when this instability reaches saturation. The toroidal field grows exponentially

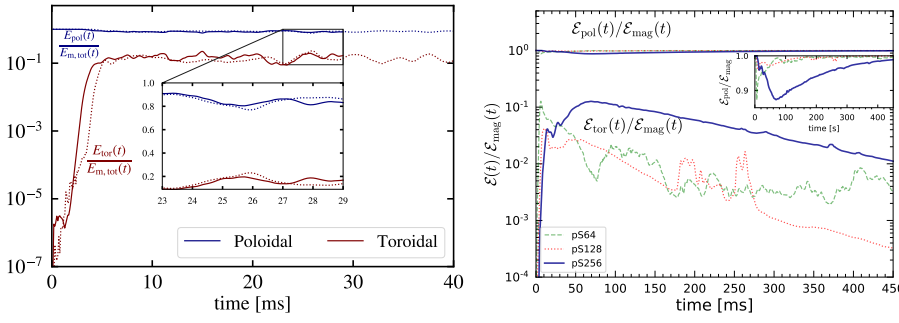

Fig. 2: Poloidal and toroidal energies at (*left*) early times from MHD setup (taken from Sur et al. (2020)) (*right*) late times with GRMHD evolution.

from its initial state until $t \sim 1$ Alfvén time are observed both inside the star and outside it. It can be seen that the strength of the toroidal field at this point becomes comparable to the poloidal field (see middle panel of the Figure 1). The field lines create vortex-like structures in the equatorial view (see right panel) due to the conservation of magnetic helicity. From $t = 12$ ms, the evolution proceeds with nonlinear rearrangement of the field, including not only the closed field lines but also the whole star. A slow evolution of the field occurs in which the interior closed field lines move outward, losing energy in its toroidal component. This will be discussed in more detail when we discuss the energies of the poloidal and toroidal components in the following section. Changing the magnetic field also expels matter from the star, but the change in rest mass ($\Delta M_{\rm rest} \approx 10^{-5} M_\odot$) is much slower than the change in magnetic field energy during the first Alfvén crossing. Field dynamics depend on the strength of the magnetic field, as stronger fields have a more violent dynamic, and vice versa (Ciolfi & Rezzolla, 2012). As a result of our simulation, we concluded that the geometry of the magnetic field has changed radically and that it has lost all traces of its original configuration. Even though we do not have resistivity, there is numerical dissipation from our grid, and it is difficult to determine if the post-instability configuration is stable. Meanwhile, the time scale on which the rest mass of a star is changing is much longer than the instabilities of the magnetic field.

3.2 Energies

We compute various energy integrals, such as the poloial and toroidal energies, and the total energies in terms of kinetic, magnetic, and enthalpy. We show two results for the evolution of magnetic field: first with MHD simulations for 40 ms, and second with GRMHD simulations for 450 ms. Figure 2 (left) shows the evolution of poloidal and the toroidal magnetic field energies normalized by the total magnetic field energy at each time for the entire run of a simulation in which the initial condition was a purely poloidal field. The toroidal component initially gains strength from the initial perturbation we gave. After 3 ms, the poloidal field becomes unstable and the toroidal component undergoes an exponential growth with its strength becoming comparable to the poloidal component. This exponential growth happends during

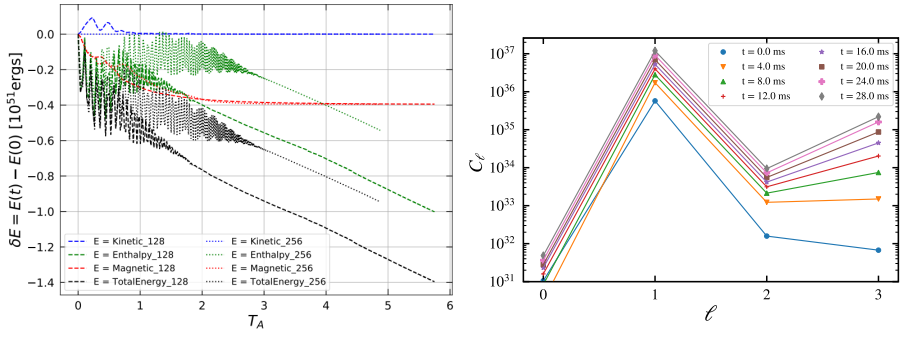

Fig. 3: The kinetic, magnetic, enthalpy and the total energies as a function of Alfvén crossing times (*left*). Power of different multipoles of the magnetic field with the MHD evolution (*right*). The figure is taken from Sur et al. (2020)

.

$t \sim 1$Alfvén timescale, where the toroidal energy becomes $\mathcal{E}_{\rm tor} \sim 0.1\mathcal{E}_{\rm mag}$. In the longer runs, as the system loses magnetic energy, the toroidal component becomes weaker and reaches approximately 1% of the total magnetic energy (Fig. 2 right panel). In this evolution, the toroidal field appears to reach a stable equilibrium with energies similar to those derived from solving the Grad-Shafranov equation for example, in Lander & Jones (2009); Armaza et al. (2015) and Sur & Haskell (2021).

In order to investigate the energetics of the star, the total energy is subdivided into four components including kinetic, magnetic, rest mass, and enthalpy. We find that the total energy remains conserved, however, the magnetic energy decays. To understand the loss of magnetic energy, we plot δE for the individual energy components (except the rest mass as it remains conserved in our simulations) inside the star and look at their behavior with time. First, the change in kinetic energy from its initial value is negligibly small. Second, the magnetic energy decreases and this loss is independent of the resolution of our simulations. More than 90% of the initial magnetic energy is lost. A major portion of it goes into heating the interior of the star as we can see from the rise in enthalpy till $\sim 2T_{\rm A}$ where $T_{\rm A}$ is defined in Sur et al. (2022). The enthalpy loss is dependent on the grid resolution and reduces by a factor two when the resolution is increased of the same factor. Higher resolutions than those considered here would be needed to minimize numerical dissipation effects. These results strongly depend on the outflow boundary conditions used in our simulations; however, realistic NS has a crystalline-solid crust, which would prevent any dissipation of magnetic energy outside the star and can significantly influence our simulation results.

We also decompose the magnetic field vector into vector spherical harmonics and calculate the power for each of the multipoles $\ell \in (0, 1, 2, 3)$. From figure the right panel of Fig. 3, we see that although initially the field is dipolar, at late times, a complex multipolar structure emerges close to the surface.

4 Discussions

In this paper we have presented the results of three dimensional MHD and GRMHD simulations of magnetic field configurations in NSs. We do not consider the effect of the crust, or of superfluidity in the interior. Our results are thus applicable to the first few hours of life of the star, after differential rotation is dissipated. The field configurations are then 'frozen in' as the star cools, and may be used as initial conditions for longer term simulations, on timescales of $10^3 - 10^5$ years, Overall we find that a NS with a given inferred dipolar field strength far from the surface, is likely to harbour an interior toroidal component with an average energy of roughly 20% of the poloidal component, but that stronger toroidal fields are unstable and cannot be sustained. We can conclude that the final configuration in our simulations is not a "strict" equilibrium but rather a "quasi-stationary" equilibrium.

Acknowledgements. AS thanks the Copernicus Astronomical Center, Warsaw, Poland for computational facilities. This project was supported by an OPUS grant from the Polish National Science Centre (NCN), No. 2018/29/B/ST9/02013.

References

Armaza, C., Reisenegger, A., Valdivia, J. A., *ApJ* **802**, 2, 121 (2015)
Bilous, A. V., et al., *ApJL* **887**, 1, L23 (2019)
Braithwaite, J., *MNRAS* **386**, 4, 1947 (2008)
Braithwaite, J., Nordlund, A., *A&A* **450**, 1077 (2006)
Chung, C. T. Y., Melatos, A., *MNRAS* **411**, 4, 2471 (2011a)
Chung, C. T. Y., Melatos, A., *MNRAS* **415**, 2, 1703 (2011b)
Ciolfi, R., Ferrari, V., Gualtieri, L., *MNRAS* **406**, 2540 (2010)
Ciolfi, R., Lander, S. K., Manca, G. M., Rezzolla, L., *ApJ* **736**, L6 (2011)
Ciolfi, R., Rezzolla, L., *ApJ* **760**, 1, 1 (2012)
Ciolfi, R., Rezzolla, L., *MNRAS* **435**, L43 (2013)
Cutler, C., *Phys. Rev. D* **66**, 084025 (2002)
Glampedakis, K., Lasky, P. D., *MNRAS* **463**, 3, 2542 (2016)
Haskell, B., Samuelsson, L., Glampedakis, K., Andersson, N., *MNRAS* **385**, 531 (2008)
Kiuchi, K., Yoshida, S., *Phys. Rev. D* **78**, 044045 (2008)
Lander, S., Jones, D., *MNRAS* **412**, 3, 1730 (2011)
Lander, S. K., Jones, D. I., *MNRAS* **395**, 4, 2162 (2009)
Lasky, P. D., *PASA* **32**, e034 (2015)
Lasky, P. D., Melatos, A., *Phys. Rev. D* **88**, 10, 103005 (2013)
Lasky, P. D., Zink, B., Kokkotas, K. D., Glampedakis, K., *ApJL* **735**, L20 (2011)
Mignone, A., et al., *ApJS* **170**, 228 (2007)
Sur, A., Haskell, B., *PASA* **38**, e043 (2021)
Sur, A., Haskell, B., Kuhn, E., *MNRAS* **495**, 1, 1360 (2020)
Sur, A., et al., *MNRAS* **511**, 3, 3983 (2022)
Thompson, C., Duncan, R. C., *ApJ* **473**, 1, 322 (1996)
White, C. J., Stone, J. M., Gammie, C. F., *ApJS* **225**, 2, 22 (2016)